

An efficient computational technique for 3D vibro-acoustic thanks to the VTTCR

Kovalevsky Louis¹, Ladevèze Pierre^{1,2}, Riou Hervé¹

¹ LMT-Cachan (ENS Cachan/CNRS/Univ. Paris 6, PRES UniverSud Paris) 61 av du Pr. Wilson, F-94230 CACHAN, France

²EADS Foundation Chair Advanced Computational Structural Mechanics

email: kovalevsky@lmt.ens-cachan.fr, ladeveze@lmt.ens-cachan.fr, riou@lmt.ens-cachan.fr

ABSTRACT: The Variational Theory of Complex Rays (VTTCR) is a wave computational approach which was proposed for the resolution of medium frequency problems. It uses a variational formulation of the problem which enables one to use any type of shape function within the substructures provided that it verifies the governing equation. Thus, the solution can be approximated using plane waves, which is very interesting in the medium-frequency vibration domain and also leads to an exponential convergence of the method. In this paper, the VTTCR is extended to the analysis of the steady-state dynamic 3D coupled vibro-acoustic problems in the mid-frequency range. It uses a specific dedicated variational formulation and a representation of the amplitude of the waves through a Fourier series (2D problems) or a Laplace series (3D problems). An illustration on a 3D vibro-acoustic example and its comparison with a FEM analysis will show the efficiency of a such an approach.

KEY WORDS: Mid-frequency vibration, vibro-acoustics coupling, Variational Theory of Complex Rays, Fourier series

1 INTRODUCTION

At present, the finite element and boundary element methods are the most commonly used techniques for solving steady-state dynamic problems. Above a certain frequency, due to the pollution errors [1], these methods would require a prohibitively large amount of computational effort and memory resources to get an acceptable level of prediction accuracy. For 3D coupled vibro-acoustic problems, the conflict between computational cost and accuracy is even more pronounced than for uncoupled problems.

In recent years, a variety of techniques have been proposed to minimise the last cited drawbacks and as a result, increase the practical application range of the FEM to higher frequencies. Among these techniques, we have the predefined reduced bases [2], the Galerkin least-squares FEM [3], the quasi-stabilized finite element method [4], the partition of unity method (PUM) [5], the generalized finite element method [6] and residual-free bubbles [7], [8]. They have all shown their capacity to reduce computational costs. However, the range of frequency solved by these methods is still lower than the mid and high-frequency range.

Apart from the FEM and all the last cited methods, there is another family of methods, the so called Trefftz methods [9], which differ from the FEMs by their choice of shape functions. Indeed, instead of using approximated functions, exact solutions of the governing differential equations are used for the expansion of the field variables. These approaches include, for example, a special use of the PUM [10], [11], the ultra-weak variational method [12], the least-squares method [13], the discontinuous enrichment method (DEM) [14], the element-free Galerkin method [15], the wave boundary element method [16] and the wave-based method [17]. The Variational Theory of Complex Rays (VTTCR), developed in this paper,

belongs also to the category of the numerical techniques which uses oscillating functions to solve the problem.

The decisive advantage of such methods (common to all Trefftz methods) is that no refined discretization is necessary, as they use exact solutions of the governing equation. Therefore, the model size and the computational effort are considerably reduced compared to element-based methods. The main differences among all these approaches is the treatment of the transmission conditions (between the sub-structures) and the boundary conditions, and the type of shape functions used.

The VTTCR is based on a variational formulation of the problem which was developed in order to enable the approximations within the subdomains to be *a priori* independent of one another and which takes into account both the boundary conditions and the continuity across the interfaces, thus eliminating the need for a specific treatment to guarantee interelement continuity (see [18]). Moreover, in each substructure, any type of shape function can be used, as soon as it verifies the governing equation. This gives to the approach a great flexibility and, consequently, efficiency. For vibration problems, the VTTCR approximates the solution through a set of plane wave functions which satisfy the governing differential equations exactly. Therefore, no residual error is involved with the governing partial differential equation inside the subdomains. However, the functions may violate the boundary conditions. Enforcing this residual boundary errors to zero thanks to the previous variational formulation yields a small matrix equation, whose solution gives the angular distribution of waves in space. In [19] and [20], the VTTCR was used to predict the vibrational response of a 3-D plate assembly. In [21], plates with heterogeneities were taken into account. In [22], this theory was extended to shell structures. The calculation of the vibrational response over a range of frequencies was presented in [23]. The use of the VTTCR for transient dynamics problems was covered in [24]. The extension to acoustic problem was made in [25] and its

adaptive version was developed in [26]. More recently, a new version of the VTCT using Fourier series has been proposed in [27]. It was shown through many examples that this approach was capable of finding an accurate solution by using few dofs.

In this paper, the VTCT is extended to the analysis of the steady-state dynamic analysis of 3D coupled vibro-acoustic systems in the mid-frequency range.

2 THE REFERENCE PROBLEM

Let $\Omega_{a,E}$ be a set of acoustic cavities, filled with a fluid, surrounded on some of their boundaries by flat and flexible plates $\Omega_{s,E}$. The unknowns of the problem are the pressure p in Ω_a , and the normal displacement w in Ω_s , and are governed by the Helmholtz equation (1) in the acoustic cavity and by the Kirchhoff equation (4) for the plate bending motion.

By sake of simplicity, let assume that the reference problem is defined on subcavities Ω_{a1} and Ω_{a2} and two uncoupled plates Ω_{s1} and Ω_{s2} . Let $\Gamma_{EE'}$ be the acoustic interface between the two acoustic cavities. The acoustic reference problem is:

Find $p_E(\underline{x})$ for $\underline{x} \in \Omega_{a,E}$ such as:

$$\Delta p_E + k_a^2 p_E = f(\underline{x}) \quad \text{in } \Omega_{a,E}, \quad E \in \{1,2\} \quad (1)$$

$$\left\{ \begin{array}{ll} p_E = p_{dE} & \text{on } \partial_p \Omega_{aE} \quad (a) \\ L_v[p_E] = v_{dE} & \text{on } \partial_v \Omega_{aE} \quad (b) \\ p_E - Z_E L_v[p_E] = h_{dE} & \text{on } \partial_Z \Omega_{aE} \quad (c) \\ L_v[p_E] = i\omega w_{E'} & \text{on } \partial_{S_{E'}} \Omega_{aE} \quad (d) \end{array} \right. \quad (2)$$

$$\left\{ \begin{array}{ll} p_E - p_{E'} = 0 & \text{on } \Gamma_{EE'} \\ L_v[p_E] + L_v[p_{E'}] = 0 & \text{on } \Gamma_{EE'} \end{array} \right. \quad (3)$$

where k_a is the acoustic wave vector, $f(\underline{x})$ a loading function, $L_v[p_E] = \frac{i}{\rho_0 \omega} \frac{\partial p_E}{\partial \underline{n}}$ the velocity operator. Boundary conditions on the boundaries of Ω_a are related to prescribed pressures (2-a), velocities (2-b), Robin equation (2-c), coupling equations in term of velocities (2-d), and interface continuity between the acoustic subcavity (3).

The plate bending reference problem is: find $w_E(\underline{x})$ for $\underline{x} \in \Omega_{s,E}$ such as:

$$\Delta \Delta w_E - k_s^4 w_E = \frac{p(\underline{x})}{D} + g(\underline{x}) \quad \text{in } \Omega_{s,E} \quad (4)$$

$$\left\{ \begin{array}{ll} w_E = w_{dE} & \text{on } \partial_w \Omega_{sE} \quad (a) \\ L_\theta[w_E] = \theta_{dE} & \text{on } \partial_\theta \Omega_{sE} \quad (b) \\ L_M[w_E] = M_{dE} & \text{on } \partial_M \Omega_{sE} \quad (c) \\ L_T[w_E] = T_{dE} & \text{on } \partial_T \Omega_{sE} \quad (d) \end{array} \right. \quad (5)$$

where k_s is the plate wave vector, $g(\underline{x})$ a loading function, D the bending stiffness of the plate, $L_\theta[w_E]$, $L_M[w_E]$ and $L_T[w_E]$ respectively the rotation, moment and shear forces operators defined on the edge of the plate Ω_{sE} by:

$$L_\theta[w_E] = \frac{\partial w_E}{\partial \underline{n}_E} \quad (6)$$

$$\underline{L}_\chi[w_E] = -\underline{\text{grad}}[\underline{\text{grad}}[w_E]] \quad (7)$$

$$L_M[w_E] = \underline{n}_E \frac{h^3}{12} \underline{K}_{PS} \underline{L}_\chi[w_E] \underline{n}_E \quad (8)$$

$$L_T[w_E] = \frac{h^3}{12} \underline{n}_E \underline{\text{div}} \left[\underline{K}_{PS} \underline{L}_\chi[w_E] \right] + \frac{h^3}{12} \frac{\partial}{\partial \underline{t}_E} \left(\underline{t}_E \underline{K}_{PS} \underline{L}_\chi[w_E] \underline{n}_E \right) \quad (9)$$

where, \underline{n}_E and \underline{t}_E are the normal and tangent unitary vector of the edge, h the thickness of the plate, and \underline{K}_{PS} the Hooke operator with plane stress condition.

Boundary conditions are related to prescribed displacements (5-a), rotations (5-b), moments (5-c) and shear forces (5-d) on the boundaries of $\Omega_{s,E}$. As one can see the coupling equations between the acoustic cavity $\Omega_{a,E}$ and the plate $\Omega_{s,E}$ are included in the inhomogeneous part of the Kirchhoff equation (4).

3 THE VARIATIONAL FORMULATION

The VTCT formulation is obtained from the boundary value problem (1-2-3-4-5) by rewriting it in a weak form. The following functional spaces $A_{ad,0}^E$, A_{ad}^E , $S_{ad,0}^E$, and S_{ad}^E required: the space of functions satisfying respectively the homogeneous and inhomogeneous Helmholtz equation in the whole sub-cavity Ω_{aE} , the homogeneous and inhomogeneous Kirchhoff equation in the whole plate Ω_{sE} :

$$A_{ad,0}^E = \{ p_E \mid \Delta p_E + k^2 p_E = 0, \forall \underline{x} \in \Omega_{aE} \} \quad (10)$$

$$A_{ad}^E = \{ p_E \mid \Delta p_E + k^2 p_E = f(\underline{x}), \forall \underline{x} \in \Omega_{aE} \} \quad (11)$$

$$S_{ad,0}^E = \{ w_E \mid \Delta \Delta w_E - k_s^4 w_E = 0, \forall \underline{x} \in \Omega_{sE} \} \quad (12)$$

$$S_{ad}^E = \{ w_E \mid \Delta \Delta w_E - k_s^4 w_E = g(\underline{x}), \forall \underline{x} \in \Omega_{sE} \} \quad (13)$$

It can be shown (see [26]) that the boundary value problem (1-2-3-4-5) is equivalent to the following variational problem: Find $(p_1, p_2, w_1, w_2) \in A_{ad}^1 \times A_{ad}^2 \times S_{ad}^1 \times S_{ad}^2$, such as:

$$\begin{aligned} & \sum_{\Omega_{aE}} \Re \left\{ \int_{\partial_p \Omega_{aE}} (p_E - p_{dE}) \overline{L_v[\delta p_E]} ds + \int_{\partial_v \Omega_{aE}} \left(\overline{L_v[p_E] - v_{dE}} \right) \delta p_E ds \right. \\ & \quad + \frac{1}{2} \int_{\partial_Z \Omega_{aE}} \left[\left((1 - Z_E L_v)[p_E] - h_{dE} \right) \overline{L_v[\delta p_E]} \right. \\ & \quad \quad \left. \left. + \left(\overline{L_v - 1/Z_E} [p_E] + h_{dE}/Z_E \right) \delta p_E \right] ds \right. \\ & \quad \left. + \int_{\partial_{S_{E'}} \Omega_{aE}} \left(\overline{L_v[p_E] - i\omega w_{E'}} \right) \delta p_E ds \right\} \\ & + \sum_{\Gamma_{EE'}} \Re \left\{ \frac{1}{2} \int_{\Gamma_{EE'}} \left((p_E - p_{E'}) \overline{L_v[\delta p_E - \delta p_{E'}]} \right. \right. \\ & \quad \left. \left. + \overline{L_v[p_E + p_{E'}]} (\delta p_E + \delta p_{E'}) \right) ds \right\} \\ & - \sum_{\Omega_{sE}} \Re \left\{ i\omega \int_{\partial_w \Omega_{sE}} \left(\overline{w_E - w_{dE}} \right) L_T[\delta w_E] dl \right. \\ & \quad + i\omega \int_{\partial_T \Omega_{sE}} \left(L_T[w_E] - T_{dE} \right) \overline{\delta w_E} dl \\ & \quad + i\omega \int_{\partial_\theta \Omega_{sE}} \left(\overline{L_\theta[w_E] - \theta_{dE}} \right) L_M[\delta w_E] dl \\ & \quad \left. + i\omega \int_{\partial_M \Omega_{sE}} \left(L_M[w_E] - M_{dE} \right) \overline{L_\theta[\delta w_E]} dl \right\} = 0 \\ & \quad \forall (\delta p_1, \delta p_2, \delta w_1, \delta w_2) \in A_{ad,0}^1 \times A_{ad,0}^2 \times S_{ad,0}^1 \times S_{ad,0}^2 \quad (14) \end{aligned}$$

This variational formulation of the reference problem is a direct extension of the formulation presented in [18], [19] and

[25], with an additional term corresponding to the coupling between the acoustic cavity and the structural plate. In case of coupled plates, there is an additional term in the variational formulation due to this coupling (see [19] and [20]).

4 EXPANSION OF THE FIELD VARIABLE

4.1 Acoustic field variable

The VTCR seeks a solution of an acoustic problem as:

$$p(\underline{x}) \approx p^p(\underline{x}) + p^h(\underline{x}), \quad p^p(\underline{x}) \in A_{ad}^E, \quad p^h(\underline{x}) \in A_{ad,0}^E \quad (15)$$

where p^p and p^h are respectively a particular solution and a homogeneous solution of (1).

For acoustic problems, the VTCR approximates the homogeneous solution through a set of plane wave functions which satisfy the governing differential equations exactly.

$$p^h(\underline{x}) = \int_{C_a} A^h(\underline{k}_a) \cdot e^{i\underline{k}_a \cdot \underline{x}} dC_a, \quad \underline{x} \in \Omega_a \quad (16)$$

where C_a corresponds to the locus of all the wave vectors \underline{k}_a such that $e^{i\underline{k}_a \cdot \underline{x}}$ satisfies (1). $A^h(\underline{k}_a)$ is the amplitude portrait. As propagative and evanescent waves are taken in account the locus C_a could be decomposed in two spaces:

- $C_{a,p}$ the locus associated to propagative plane waves. In spherical coordinates $((\underline{e}_r, \underline{e}_\theta, \underline{e}_\varphi), \theta \in [-\frac{\pi}{2}, \frac{\pi}{2}], \varphi \in [0, 2\pi])$, this space correspond to the unit sphere, the wave vector is defined as

$$\underline{k}_a^p = ik_a \underline{e}_r \quad (17)$$

The amplitude portrait $A^{h,p}(\theta, \varphi)$ is a function defined over the unit sphere, and is discretized as a Laplace serie, *i.e.* using spherical harmonics $Y_l^m(\theta, \varphi)$.

$$A^{h,p}(\theta, \varphi) = \sum_{l=0}^{L_p} \sum_{m=-l}^l a_{l,m}^p \int_{-\pi/2}^{\pi/2} \int_0^{2\pi} Y_l^m(\theta, \varphi) \sin(\varphi) d\theta d\varphi \quad (18)$$

with

$$Y_l^m(\theta, \varphi) = \sqrt{\frac{2 \cdot (l-m)!}{(l+m)!}} \cdot P_l^m(\cos\theta) \cdot e^{im\varphi} \quad (19)$$

$$P_l^m(X) = \frac{(-1)^m}{2^l \cdot l!} (1-X^2)^{m/2} \frac{\partial^{m+l}(X^2-1)^l}{\partial X^{m+l}}$$

where, $Y_l^m(\theta, \varphi)$ is the spherical harmonics of non negative index l and of momentum m , (m varies from $-l$ to l). $P_l^m(X)$ is the Legendre polynomial.

- $C_{a,e}$ the locus associated to evanescent plane waves. To be able to represent the physic, all evanescent waves with a wavelength larger than the structural wave length have to be considered. Let \underline{n} , $\underline{\tau}_1$, and $\underline{\tau}_2$ be the normal and two tangent vectors of an edge of the acoustic cavity making an orthogonal basis. The wave vector of the evanescent plane wave associated to this edge could be defined as:

$$\underline{k}_a^e = k_a \sqrt{1 + \left(\frac{k_s}{k_a} \cos(\theta)\right)^2} \underline{n} + ik_s \cos(\theta) (\cos(\varphi) \underline{\tau}_1 + \sin(\varphi) \underline{\tau}_2) \quad (20)$$

The amplitude portrait $A^{h,e}$ is a function defined over the unit sphere, and is discretized as a Laplace serie

$$A^{h,e}(\theta, \varphi) = \sum_{l=0}^{L_e} \sum_{m=-l}^l a_{l,m}^e \int_{-\pi/2}^{\pi/2} \int_0^{2\pi} Y_l^m(\theta, \varphi) \sin(\varphi) d\theta d\varphi \quad (21)$$

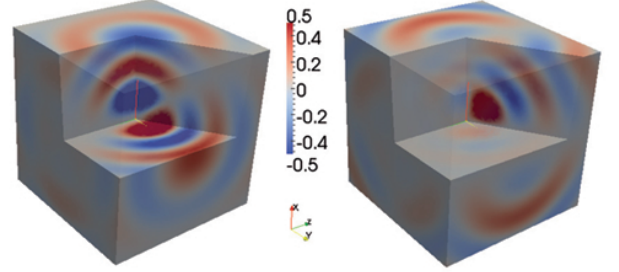


Figure 1. Real (left) and imaginary (right) part of the pressure field associated to the interior shape function $\Phi_{2,-2}^{a,p}(\underline{x})$ in a cubic cavity filled with air.

The homogeneous part of the acoustic approximation is:

$$\begin{aligned} p^h(\underline{x}) &= \int_{-\pi/2}^{\pi/2} \int_0^{2\pi} A^{h,p}(\theta, \varphi) \cdot e^{i\underline{k}_a^p(\theta, \varphi) \cdot \underline{x}} \sin(\varphi) d\theta d\varphi \\ &+ \int_{-\pi/2}^{\pi/2} \int_0^{2\pi} A^{h,e}(\theta, \varphi) \cdot e^{i\underline{k}_a^e(\theta, \varphi) \cdot \underline{x}} \sin(\varphi) d\theta d\varphi \\ &= \sum_{l=0}^{L_p} \sum_{m=-l}^l a_{l,m}^p \int_{-\pi/2}^{\pi/2} \int_0^{2\pi} Y_l^m(\theta, \varphi) e^{i\underline{k}_a^p(\theta, \varphi) \cdot \underline{x}} \sin(\varphi) d\theta d\varphi \\ &+ \sum_{l=0}^{L_e} \sum_{m=-l}^l a_{l,m}^e \int_{-\pi/2}^{\pi/2} \int_0^{2\pi} Y_l^m(\theta, \varphi) e^{i\underline{k}_a^e(\theta, \varphi) \cdot \underline{x}} \sin(\varphi) d\theta d\varphi \\ &= \sum_{l=0}^{L_p} \sum_{m=-l}^l a_{l,m}^p \Phi_{l,m}^{a,p}(\underline{x}) + \sum_{l=0}^{L_e} \sum_{m=-l}^l a_{l,m}^e \Phi_{l,m}^{a,e}(\underline{x}) \end{aligned} \quad (22)$$

Some examples of these Laplace-based functions are shown in Figures 1 and 2. As one can see, the wavelength of the evanescent waves is smaller than the propagative ones.

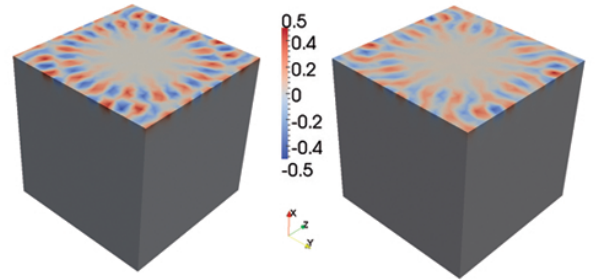


Figure 2. Real (left) and imaginary (right) part of the pressure field associated to the evanescent shape function $\Phi_{3,-3}^{a,e}(\underline{x})$ in a cubic cavity filled with air.

4.2 Structural field variable

The VTCR seeks a solution of a structural vibrational problem as:

$$w(\underline{x}) \approx w^p(\underline{x}) + w^h(\underline{x}), \quad w^p(\underline{x}) \in S_{ad}^E, \quad w^h(\underline{x}) \in S_{ad,0}^E \quad (23)$$

where w^p and w^h are respectively a particular solution and a homogeneous solution of (4).

Due to the approximation of the acoustic field, the solution w^p is a combinaison of the elementary solution resulting from one of the acoustic wave functions Φ^a in the cavity pressure expansion and a contribution from the loading function $g(\underline{x})$. Due to the flat shape of the plate, a particular solution function for last first contribution may be defined, which is proportional to the pressure loading function:

$$w^p(\underline{x}) = \frac{\Phi^a(\underline{x})}{D((\underline{k}_a \cdot \underline{\tau}_1)^4 + (\underline{k}_a \cdot \underline{\tau}_2)^4 + 2(\underline{k}_a \cdot \underline{\tau}_1)^2(\underline{k}_a \cdot \underline{\tau}_2)^2 - k_s^4)} \quad (24)$$

For vibration problems, the VTCR approximates the homogeneous solution through a set of plane wave functions which satisfy the governing differential equations exactly.

$$w^h(\underline{x}) = \int_{C_s} B^h(\underline{k}_s) \cdot e^{i\underline{k}_s \cdot \underline{x}} dC_s, \quad \underline{x} \in \Omega_s \quad (25)$$

where C_s corresponds to the locus of all the wave vectors \underline{k}_s such that $e^{i\underline{k}_s \cdot \underline{x}}$ satisfies (4), $B^h(\underline{k}_s)$ is the amplitude portrait.

As propagative and evanescent waves are taken in account, the locus C_s could be decomposed in two sub spaces:

- $C_{s,p}$ the locus associated to propagative plane waves. In the polar coordinate associated to the plate $((\underline{e}_r, \underline{e}_\theta), \theta \in [0, 2\pi[)$, this space corresponds to the unit circle, and the wave vector is:

$$\underline{k}_s^p = ik_s \underline{e}_r \quad (26)$$

The amplitude portrait $B^{h,p}(\theta)$ is a function defined over the unit circle, and is discretized as a Fourier serie.

$$B^{h,p}(\theta) = \sum_{n=-N_p}^{N_p} b_n^p \int_0^{2\pi} e^{in\theta} d\theta \quad (27)$$

- $C_{s,e}$ the locus associated to evanescent plane waves. The wave vector could be defined as

$$\underline{k}_s^e = k_s \sqrt{1 + \cos(\theta)^2} \underline{n} + ik_s \cos(\theta) \underline{\tau}, \quad \theta \in [0, 2\pi] \quad (28)$$

where $\underline{\tau}$ and \underline{n} are the tangent and normal vectors of one edge of the plate. The amplitude portrait $B^{h,e}$ is a function defined over the unit circle, and is also discretized as a Fourier serie.

The homogeneous part of the structural approximation is:

$$\begin{aligned} w^h(\underline{x}) &= \int_0^{2\pi} B^{h,p}(\theta) \cdot e^{i\underline{k}_s^p(\theta) \cdot \underline{x}} d\theta + \int_0^{2\pi} B^{h,e}(\theta) \cdot e^{i\underline{k}_s^e(\theta) \cdot \underline{x}} d\theta \\ &= \sum_{n=-N_p}^{N_p} b_n^p \int_0^{2\pi} e^{in\theta} e^{i\underline{k}_s^p \cdot \underline{x}} d\theta + \sum_{n=-N_e}^{N_e} b_n^e \int_0^{2\pi} e^{in\theta} e^{i\underline{k}_s^e \cdot \underline{x}} d\theta \\ &= \sum_{n=-N_p}^{N_p} b_n^p \Phi_n^{s,p}(\underline{x}) + \sum_{n=-N_e}^{N_e} b_n^e \Phi_n^{s,e}(\underline{x}) \end{aligned} \quad (29)$$

Some examples of these Fourier-based functions are shown in Figure 3 and 4.

As one can see, the VTCR discretizes only the amplitudes of the waves, not their spatial shapes. In that sense, the VTCR belongs to the category of the multiscale numerical approaches because it discretizes only the slowly oscillating quantities and

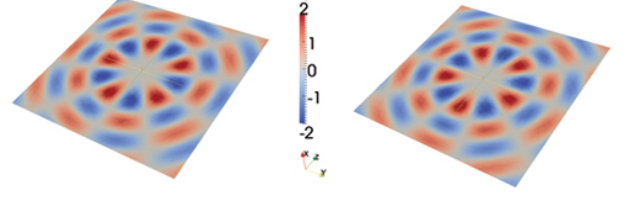


Figure 3. Real (left) and imaginary (right) part of the displacement field associated to the interior shape function $\Phi_{-5}^{s,p}(\underline{x})$.

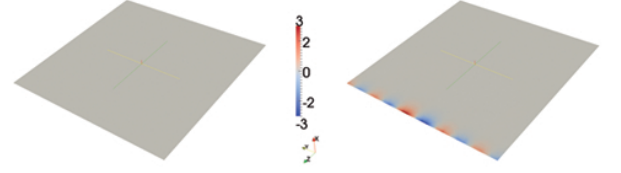


Figure 4. Real (left) and imaginary (right) part of the displacement field associated to the evanescent shape function $\Phi_2^{s,e}(\underline{x})$.

not the rapidly oscillating quantity $e^{i\underline{k}(\theta) \cdot \underline{x}}$. Finally, one can note that all the propagating waves are taken into account since the spatial repartition of the waves are represented by an integral over the space variable (and not by a discrete sum which would select only a few propagation directions). This is important because the direction of the propagation of the waves is not known *a priori*.

5 COMPUTATIONAL ASPECT

Seeking an approximate solution $(p \times w) \in (A_{ad}^{E,h} \times S_{ad}^{E,h})$ to the variational formulation (14) requires the resolution of the finite-dimension matrix system:

$$\begin{bmatrix} \mathbf{K}_{1,1}^{aa} & \mathbf{K}_{1,2}^{aa} & \cdots & \mathbf{K}_{1,1}^{as} & \mathbf{K}_{1,2}^{as} & \cdots \\ \mathbf{K}_{2,1}^{aa} & \mathbf{K}_{2,2}^{aa} & \cdots & \mathbf{K}_{2,1}^{as} & \mathbf{K}_{2,2}^{as} & \cdots \\ \vdots & \vdots & \ddots & \vdots & \vdots & \ddots \\ \mathbf{K}_{1,1}^{sa} & \mathbf{K}_{1,2}^{sa} & \cdots & \mathbf{K}_{1,1}^{ss} & \mathbf{K}_{1,2}^{ss} & \cdots \\ \mathbf{K}_{2,1}^{sa} & \mathbf{K}_{2,2}^{sa} & \cdots & \mathbf{K}_{2,1}^{ss} & \mathbf{K}_{2,2}^{ss} & \cdots \\ \vdots & \vdots & \ddots & \vdots & \vdots & \ddots \end{bmatrix} \begin{bmatrix} \mathbf{a}_1 \\ \mathbf{a}_2 \\ \vdots \\ \mathbf{b}_1 \\ \mathbf{b}_2 \\ \vdots \end{bmatrix} = \begin{bmatrix} \mathbf{f}_1^a \\ \mathbf{f}_2^a \\ \vdots \\ \mathbf{f}_1^s \\ \mathbf{f}_2^s \\ \vdots \end{bmatrix} \quad (30)$$

where $\mathbf{K}_{i,j}$ and \mathbf{f}_i are respectively the matrices of the bilinear forms and the vectors of the linear form of the variational formulation (14) calculated for all the test functions. \mathbf{a}_i is the vector of the amplitudes of the shape functions used in the acoustic cavities; \mathbf{b}_i is the vector of the amplitudes of the shape functions used in the plates.

Since the shape functions used are defined over the entire subdomain Ω_E , the matrices of the model are fully populated. However, in the case of more than two subdomains, if subdomain i is not connected to subdomain j the corresponding off-diagonal submatrix $\mathbf{K}_{i,j}$ is zero.

Due to the expression of the approximation in the plates, the terms of the variational formulation (14) associated to the

boundaries conditions of the plates S_E have contribution in \mathbf{K}_{EE}^{SS} if the plate is not coupled with a cavity, but otherwise also in $\mathbf{K}_{EE'}^{sa}$, $\mathbf{K}_{E'E}^{as}$, and $\mathbf{K}_{E'E'}^{aa}$ if coupled with the cavity $\Omega_{E'}$.

The calculation of the matrix coefficients involves the integration of highly oscillatory functions. Special care must be taken in carrying out these integrations in order to ensure good convergence. The integration is done in two steps:

- evaluation of the shape functions $\Phi(\underline{x})$ over the edges,
- computation of the matrix coefficients through a classic Simpson scheme.

In the case of propagative waves with no internal damping, the Angers Jacobi expansion [28] gives an analytical result of the first step.

Graphics Processing Units (GPU) or parallel computing with multiple servers can also be used to accelerate many of the computations without resorting to low-level programming

6 APPLICATION CASE

Finally, we present an application of the Fourier VTCR to a three-dimensional vibro-acoustic problem. The computed example is used to determine the transmission coefficient of a plate between two acoustic cavities filled with air.

Let us consider two cubic ($1 \text{ m} \times 1 \text{ m} \times 1 \text{ m}$) cavities filled with air ($\rho = 1.25 \text{ kg.m}^{-3}$ and $c = 330 \text{ m.s}^{-1}$) separated with an undamped 3 mm thick iron plate ($\rho = 7870 \text{ kg.m}^{-3}$, $E = 200 \text{ MPa}$ and $\nu = 0.29$). The two cavities are bounded by rigid walls, except for the left-hand-side one, on which a constant unitary pressure is apply. This problem is solved at three frequencies $f = 500, 750$ and 1000 Hz .

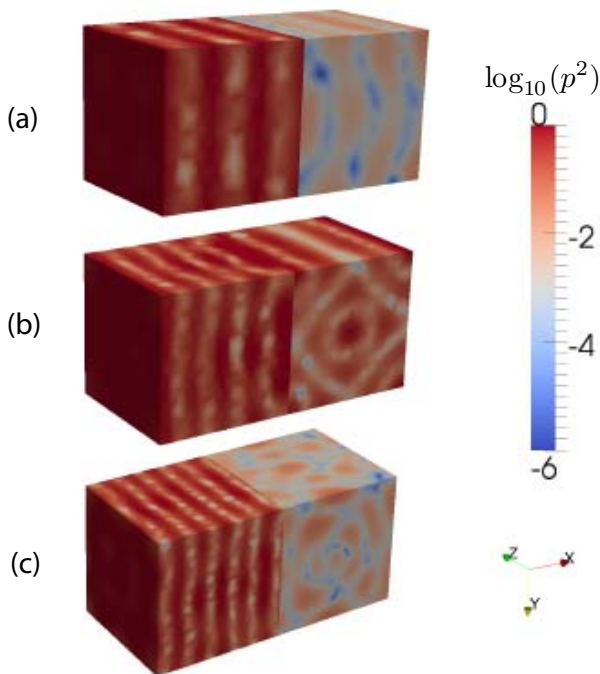


Figure 5. Sound pressure level (dB) in the two cavities for the three frequencies 500 Hz (a), 750 Hz (b) and 1000 Hz (c).

Let p_1 and p_2 be respectively the average quadratic pressure in the first and second cavity, the transmission coefficient τ of

the plate is defined as:

$$\tau = \log_{10} \left(\frac{p_2}{p_1} \right) \quad (31)$$

For each frequency, the performances of the VTCR software CoFouRays are compared to the commercial software Comsol, in terms of CPU time and needed memory.

These computations have been done on a Carri system computer with 2 Xeon 6 core 2.66 GHz processors, 72 Gb of RAM, and 8 Tesla C1060 GPU. Figure 5 shows the map of sound pressure level obtained with the VTCR, the 3D coarse mesh is only used to represent the solution.

The comparaisons are presented in table 1. As one can see, for the first two frequencies, the results between the commercial software and the VTCR one are very closed. For the highest frequency, Comsol was unable to find a solution due to an "out of memory" error.

Table 1. Transmission coefficient computed by Comsol and CoFouRays.

Frequency Hz	τ COMSOL	τ CoFouRays	relative error
500	-4.6520	-4.6709	0.41 %
750	-1.2904	-1.2810	0.73 %
1000	Out of memory	-4.6750	—

Tables 2 shows the memory needed by the two softwares to solve the problem.

Table 2. Memory needed by Comsol and CoFouRays.

Frequency Hz	Memory needed by COMSOL	Memory needed by CoFouRays
500	41 Gb	7 Gb
750	65 Gb	9 Gb
1000	Out of memory	12 Gb

As one can see, for similar precision, the CoFouRays software uses seven times fewer memory than Comsol. This first present study shows the potential of the VTCR on such problems, so programming improvements can be done with CoFouRays.

7 CONCLUSION

This paper describes the extension of the VTCR to the steady-state dynamic analysis of 3D vibro-acoustic problems, using shape functions based on the Fourier series and Laplace series expansion of the amplitudes of the plane waves traveling inside a plate or an acoustic cavity. The example solved shows the capacity of the VTCR to solve this kind of problems. Moreover, the VTCR seems to be more efficient than the classic finite element method in terms of CPU times and memory needed. Some foregoing future problems are these one: optimization of the degree of discretization, and extension to more complex problems such as coupled plates or infinite acoustic media.

ACKNOWLEDGMENTS

The authors gratefully acknowledge the ITN Marie Curie project GA-214909 "MID-FREQUENCY - CAE Methodologies for Mid-Frequency Analysis in Vibration and Acoustics".

REFERENCES

- [1] A. Deraemaeker, I. Babuska and P. Bouillard, Dispersion and pollution of the FEM solution for the Helmholtz equation in one, two and three dimensions. *International Journal in Numerical Methods in Engineering*, 46 : 471-499, 1999.
- [2] C. Soize. Reduced models in the medium frequency range for the general dissipative structural dynamic systems. *European Journal of Mechanics and A/Solids*, 17:657-685, 1998.
- [3] I. Harari and T.J.R. Hughes. Galerkin/least-squares finite element methods for the reduced wave equation with non- reflecting boundary conditions in unbounded domains, *Computer Methods in Applied Mechanics and Engineering*, 98(3):411-454, 1992.
- [4] I. Babuska, F. Ihlenburg, E.T. Paik, and S.A. Sauter. A generalized finite element method for solving the helmholtz equation in two dimensions with minimal pollution. *Computer Methods in Applied Mechanics and Engineering*, 128:325-359, 1995.
- [5] J.M. Melenk and I. Babuska. Approximation with harmonic and generalized harmonic polynomials in the partition of unity method. *Computer Assisted Mechanics and Engineering Sciences*, 4:607-632, 1997.
- [6] T. Strouboulis, K. Copps, and I. Babuska. The generalized finite element method: an example of its implementation and illustration of its performance, *International Journal for Numerical Methods in Engineering*, 47:1401-1417, 2000.
- [7] T.J.R. Hughes. Multiscale phenomena: Greens functions and the dirichlet-to-neumann formulation and subgrid scale models and bubbles and the origins of stabilized methods, *Computer Methods in Applied Mechanics and Engineering*, 127(1-4):387-401, 1995.
- [8] L.P. Franca, C. Farhat, A.P. Macedo and M. Lesoinne, Residual-free bubbles for the helmholtz equation, *International Journal for Numerical Methods in Engineering*, 40:4003-4009, 1997.
- [9] E. Trefftz, Ein gegenstück zum ritzschen verfahren, in: *Second International Congress on Applied Mechanics*, Zürich, Switzerland, 1926, pp. 131-137.
- [10] O. Laghrouche and P. Bettess, Short wave modelling using special finite elements, *Journal of Computational Acoustics*, 8(1):189-210, 2000.
- [11] T. Strouboulis and R. Hidajat, Partition of unity method for helmholtz equation: q-convergence for plane-wave and wave- band local bases, *Applications of Mathematics*, 51(2):181-204, 2006.
- [12] O. Cessenat and B. Despres, Application of an ultra weak variational formulation of elliptic pdes to the two-dimensional helmholtz problem, *SIAM Journal on Numerical Analysis*, 35(1):255-299, 1998.
- [13] P. Monk and D.Q. Wang, A least-squares method for the helmholtz equation, *Computer Methods in Applied Mechanics and Engineering*, 175:121-136, 1999.
- [14] C. Farhat, I. Harari, and L.P. Franca, The discontinuous enrichment method, *Computer Methods in Applied Mechanics and Engineering*, 190:6455-6479, 2001.
- [15] P. Bouillard and S. Suleau, Element-free galerkin solutions for helmholtz problems: formulation and numerical assessment of the pollution effect, *Computer Methods in Applied Mechanics and Engineering*, 162(1-4):317-335, 1998.
- [16] E. Perrey-Debain, J. Trevelyan, and P. Bettess, Wave boundary elements: a theoretical overview presenting applications in scattering of short waves, *Engineering Analysis with Boundary Elements*, 28(2):131-141, 2004.
- [17] W. Desmet, P. Sas and D. Vandepitte, An indirect trefftz method for the steady-state dynamic analysis of coupled vibro- acoustic systems, *Computer Assisted Mechanics and Engineering Sciences*, 8:271-288, 2001.
- [18] P. Ladevèze, A new computational approach for structure vibrations in the medium frequency range, *Comptes Rendus Acadmie des Sciences Paris*, 322(IIb):849-856, 1996.
- [19] P. Ladevèze, L. Arnaud, P. Rouch and C. Blanzé, The variational theory of complex rays for the calculation of medium- frequency vibrations, *Engineering Computations*, 18(1-2):193-214, 2001.
- [20] R. Rouch and P. Ladevèze, The variational theory of complex rays: a predictive tool for medium-frequency vibrations, *Computer Methods in Applied Mechanics and Engineering*, 192(28-30):3301-3315, 2003.
- [21] P. Ladevèze, L. Blanc, P. Rouch and C. Blanzé. A multiscale computational method for medium-frequency vibrations of assemblies of heterogeneous plates, *Computers and Structures*, 81:1267-1276, 2003.
- [22] H. Riou, P. Ladevèze and P. Rouch, Extension of the variational theory of complex rays to shells for medium-frequency vibrations, *Journal of Sound and Vibration*, 272(1-2):341-360, 2004.
- [23] P. Ladevèze, P. Rouch, H. Riou and X. Bohineust, Analysis of medium-frequency vibrations in a frequency range, *Journal of Computational Acoustics*, 11(2):255-284, 2003.
- [24] P. Ladevèze and M. Chevreuril, A new computational method for transient dynamics including the low- and the medium- frequency ranges, *International Journal for Numerical Methods in Engineering*, 64(4):503-527, 2005.
- [25] H. Riou, P. Ladevèze and B. Sourcis, The multiscale VTCR approach applied to acoustics problems, *Journal of Computational Acoustics*, 16(4):487-505, 2008.
- [26] H. Riou, P. Ladevèze, B. Sourcis, B. Faverjon and L. Kovalevsky, An adaptive numerical strategy for the medium-frequency analysis of Helmholtz's problem, submitted.
- [27] L. Kovalevsky, P. Ladevèze and H. Riou. The Variational Theory of Complex Rays for Helmholtz equation: effect of choice of Fourier series, submitted.
- [28] D. Colton and R. Kress, *Inverse Acoustic and Electromagnetic Scattering Theory*, Springer-Verlag, 1992.